

Estimating the impact of COVID-19 vaccines allocation inequalities: a modeling study

Nicolò Gozzi¹, Matteo Chinazzi², Nicola Perra^{1,2}, Alessandro Vespignani²

¹ Networks and Urban Systems Centre, University of Greenwich, UK

² Laboratory for the Modeling of Biological and Socio-technical Systems, Northeastern University, Boston, MA USA

January 16, 2022

Abstract

The access to COVID-19 vaccines on the global scale has been drastically impacted by structural socio-economic inequalities, resulting in the fact that most COVID-19 vaccines have been used in high and upper middle income countries. Here, we develop a data-driven age-stratified epidemic model to evaluate the effects of COVID-19 vaccine inequalities in eight low and middle income countries sampled from all regions of the world. The model accounts for vaccination data, non-pharmaceutical interventions, and the introduction of more transmissible strains. The modeling approach allows us the exploration of counterfactual scenarios where we either apply vaccination rates observed in high income countries or anticipate the rollout starting dates to match those of high income countries. We estimate that more than 50%, with peaks of 80%, of deaths would have been averted with respect to the actual vaccine allocation and distribution occurred in the analyzed countries. Overall, our results quantify the negative impacts of vaccines inequalities and call for the multiplication of global efforts to provide better access and support to COVID-19 vaccines in low and middle income countries.

Introduction

The scale of the COVID-19 pandemic, the socio-economic disruptions induced by the virus and by non-pharmaceutical interventions (NPIs) have exacerbated structural inequalities in access to key health tools such as vaccines [1–4]. Furthermore, socio-economic disparities have been linked to higher and disproportionate COVID-19 burden [5–13]. In the case of vaccine allocation the differences, in terms of COVID-19 vaccines doses administered across countries grouped by income levels, are staggering [14], and have potentially enormous effect on the future health, economic, and other harms due to COVID-19 [1, 2]. As of December 1st 2021, the median share of fully vaccinated individuals living in high and upper middle income countries is 60%. The equivalent share in low and lower middle income countries (LMIC) is 12%. At the same time, the share of doses administered in high and upper middle income countries is 72% against 27% in middle and less than 1% low income countries. It is important to notice how these disparities were drastically more pronounced in the early months of 2021, at the start of the vaccination campaigns (outside China, which started vaccinating much earlier in July 2020). By the end of February 2021 for example, 77% of doses were concentrated in high-income countries. Only in June 2021, the global share of doses administered in such rich countries went below 50%. Hence, for about six months more than 50% of the doses administered globally have been concentrated in 18% of the global population which lives in high-income countries.

Here, we develop a realistic, stochastic, multi-strains compartmental epidemic model to study the potential impact of less unequal vaccination campaigns in eight LMIC countries sampled from different regions of the world. In particular, we focus on Bangladesh, Bolivia, Indonesia, Kenya, Morocco, Mozambique, Sri Lanka, and Ukraine. The sampling process was driven also by data availability about vaccinations, genomics information about variants prevalence, NPIs, and reported deaths. The model accounts for demographics, age-structured contact mixing patterns, and their variations due to NPIs as well as multiple virus strains and their effects on vaccines’ efficacy. We fit the model, independently, in each country, by using an Approximate Bayesian Approximation method [15, 16]. We explore a range of counterfactual scenarios aimed at quantifying what could have happened in less unequal settings. In

the case that these countries would have been able to vaccinate at the same rate as Italy, the United Kingdom (UK), or the United States (US), we estimate that the fraction of averted deaths with respect to the actual vaccine rollout would have been larger than 50% with peaks of 80%. In case instead, these countries would have been able to start their vaccination campaigns at the same time as the European Union (27th of December, 2020) we find an overall beneficial effect with peaks of around 50% averted deaths respect to the factual analysis.

We also estimate the level of NPIs that these countries would have to put in place to offset the unequal allocation of vaccines. In fact, for the large part of 2020, the mitigation of the pandemic was achieved at high costs through the implementation of economically and socially disruptive NPIs [17], while in high-income countries, vaccines have allowed relaxing such tough socio-economic measures reopening society [18, 19]. Hence, we estimate the variation in NPIs strictness necessary to reduce the fatality burden without boosting vaccinations. We find that significantly stronger NPIs (i.e., either tougher or more prolonged) would be needed in order to achieve the same number of averted deaths estimated in the presence of the same vaccines availability of high income countries.

Overall, the results highlight the negative effects of vaccine inequalities and call for targeted efforts to provide faster and more equitable access to vaccines. This is not just a moral imperative to reduce the burden of COVID-19 around the world, but also a pragmatic stand to limit the emergence, spread, and introductions of new variants possibly able to breach the protection of existing vaccines. Though we have focused on a sample of eight LMIC countries, the approach we developed could be used to study and quantify the impact of vaccines inequality in others.

Results

In order to quantify the vaccine allocation volume and timeline of their administration across countries with different income levels, we combine two datasets. The first is managed, maintained, and disseminated by the United Nations Development Programme via their Global Futures Platform [14]. It provides general information about the COVID-19 vaccine rollout around the world, including several socio-economic dimensions. The second dataset comes from Our World in Data [20]. Besides a range of general information about the vaccination efforts around the world, it provides the number of doses administered across countries as a function of time.

In Figure 1-A we plot the number of total doses administered per 100 people. As of December 1st, 2021, high and upper middle income countries have, on average, more than one dose per person. The numbers are radically different in LMIC. While lower middle countries managed to administer slightly more than 60 doses per 100, the equivalent number for low income countries is only 9.6 per 100. The evident levels of inequality become even more staggering when considering the share of global populations of the four groups. As mentioned above, only 18% of the population lives in high income countries, while nearly 50% in LMIC.

In Figure 1-B we show a scatter plot of the Human Development Index (HDI) on the x-axis and the percentage of the fully vaccinated population of each country on the y-axis. The size of data points is set proportional to the estimated cost of vaccinating 40% of the population as a percentage of current healthcare spending. The colors indicate the income group of each country. The HDI is a composed index that accounts for life expectancy, education, and per capita income as well as other aspects of human development [21]. The cost of reaching a given vaccination level as a percentage of the healthcare spending instead is used to quantify the economic challenge posed by the COVID-19 vaccination. The plot shows a positive correlation between HDI and vaccination coverage (Pearson correlation coefficient: 0.83, $p < 0.001$). The more developed the country, the higher the fraction of its population vaccinated. Furthermore, countries characterized by the lowest values of HDI face drastically different economic challenges in reaching 40% of the population vaccinated. It is important to note how this threshold is a very low bar of immunity, far from the current levels in many high-income countries. The plot suggests that without global efforts and initiatives, countries characterized by low HDI might not be able to reach significant vaccination coverage.

In Figure 1-C we plot the distribution of vaccine rollout starting dates. As clear from the plot, the median start for high and upper middle income countries is much early than for LMIC. The difference between the peaks of high and low income countries is of about four months. This plot speaks to the differential power among income levels to secure a scarce resource such as COVID-19 vaccines in the early phases of the rollout. Furthermore, it speaks to the different capabilities and opportunities in setting up a mass vaccination campaign.

COVID-19 Vaccine Inequalities

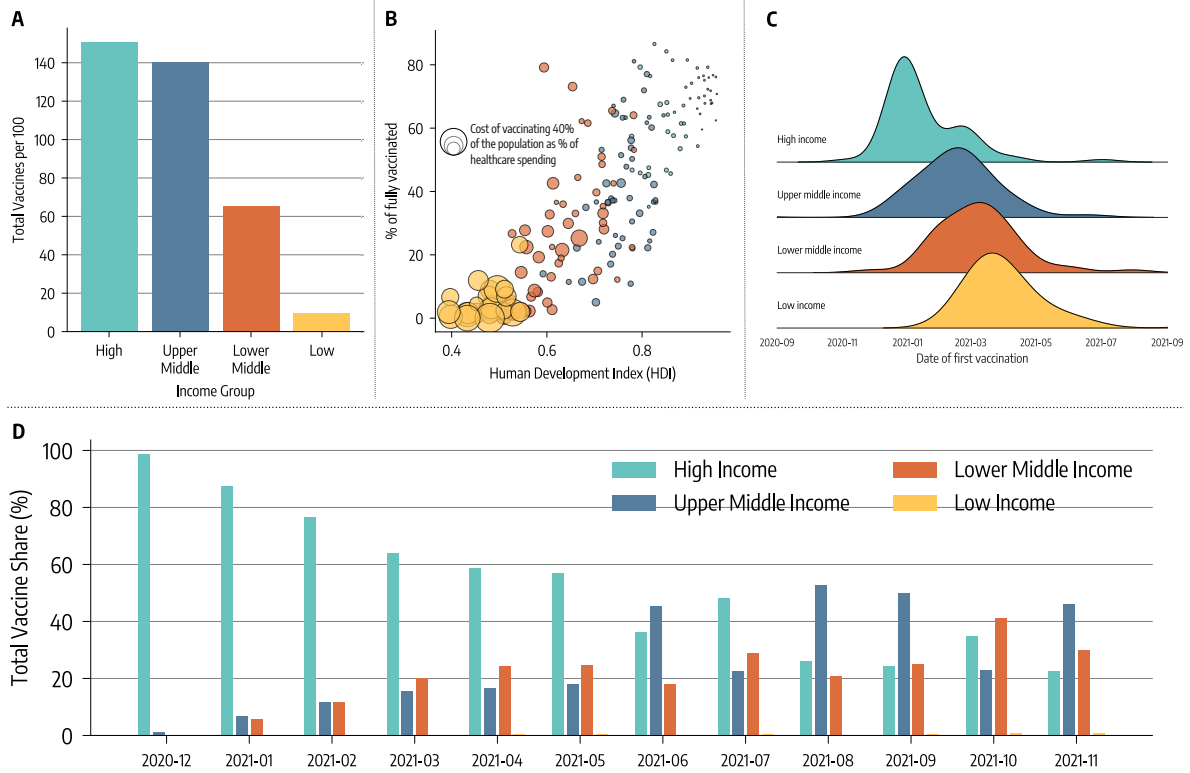


Figure 1: **Vaccine inequalities.** A) Total number of doses administered per 100 people in different income groups as of December 1st, 2021. B) Scatter plot of % of fully vaccinated versus Human Development Index (HDI) of different countries. The color of dots indicates the income group while size it is proportional to the cost of vaccinating 40% of the population expressed as percentage of current healthcare spending. C) Density plot of date of first COVID-19 vaccination across different income groups. D) Evolution in time of share of vaccines administered monthly among income groups.

In Figure 1-D, we plot the share of vaccines administered across income levels as a function of time. The trends are extremely clear and confirm how, in the first six months from the start of the COVID-19 vaccination, high income countries administered more than half of the doses globally. These figures do not consider the very early start of the rollout in China which took place in July 2020. The plot also highlights how low income countries, despite counting for 8% of the global population, have administered a share of doses that is smaller than 1% of total doses administered so far.

To quantify the potential impact of inequalities in vaccination allocation, we developed a realistic, stochastic, multi-strain, and compartmental epidemic model. The model takes as input demographics, age-stratified contact patterns, NPIs, genomics information, vaccines, and epidemic data (see the Supplementary Information for details). We fit the model calibrating it to the context and data of each country separately via an Approximate Bayesian Computation method [15]. This allows defining posterior distributions for a range of parameters such as the transmissibility of the different strains, seasonality, delay between deaths and their notification, under-reporting of deaths, infection fatality rates (IFRs) rescaling with respect to the estimates reported in Ref. [22] in high and upper middle income countries. We refer the reader to the Supplementary Information for the details about the model and the calibration process.

We use the model to study, via a series of counterfactual scenarios, what could have happened in case of i) different vaccine allocation scenarios and ii) an earlier start of the rollout of the vaccination campaign in the countries under investigation. Furthermore, we estimate the variation in strictness of NPIs necessary to offset the lack of vaccines.

In Figure 2-A, we show the percentage of averted deaths in the eight countries in case they would have been able to vaccinate with the rate of three high-income countries taken as reference: Italy, the

UK, and the US. In administering the extra doses, we assume a protocol that prioritizes the elderly population hence targeting a reduction of deaths rather than of overall infections [23–25]. In all Figures we arrange countries according to their vaccination coverage. As shown in Supplementary Information, there are marked differences in the group. We go from fractions of fully vaccinated above 50% in Sri Lanka (top left) to values below 10% in Kenya and Mozambique (bottom right). Indonesia and Bolivia are in between these two groups with a fraction of fully vaccinated population close to 20%. The percentages in the Figure are calculated with respect to the number of deaths observed in their actual vaccination campaign (see the Supplementary Information for more details). Hence, the plot describes what additional impact vaccines could have had in case these LMIC could afford the vaccine rollout of high income countries. While the vaccine availability in the UK, Italy and the US followed different timelines (see the Supplementary Information for details), the Figure shows how higher vaccination rates would have induced a very significant reduction in deaths. Numbers are above 80% for Indonesia, Sri Lanka, and Bangladesh for a rollout equivalent to the UK. The numbers are smaller but still very significant for Kenya, Mozambique, and Ukraine. Remarkably, except for Ukraine (in the case of a vaccination rate equivalent to Italy), all numbers are around or well above 50%.

Figure 2-B shows the evolution of the number of weekly deaths in the different countries under several vaccination scenarios. We show the weekly deaths as reported by surveillance (blue dots), as simulated by our model following the actual vaccination campaigns (blue solid lines and shaded areas) and the counterfactual vaccination rates of Italy (light blue), the UK (orange), and the US (light red). First, we notice a good accordance between reported and simulated deaths. This indicates that our model is able to reproduce realistically the epidemic unfolding in different countries. Second, the plot confirms the impressive impact that vaccination rates of high income countries would have had on the death toll. Indeed, the curves start to visibly diverge since 2021/04 and we observe that higher vaccination rates would have substantially avoided the waves observed in the second half of the year. As observed above, the rates of the UK and the US seems to bring additional benefit with respect to vaccination rates of Italy, nonetheless the difference with the actual vaccination rates remains unbridgeable. The results of Fig. 2-B also explains the *lower* percentage of averted deaths achieved with high-income vaccination rates in Ukraine as shown in Fig. 2-A. A new, massive wave fuelled by the Delta VOC started in Ukraine in late August, 2021. The number of reported deaths peaked in mid November 2021, with twice as much fatalities as those reported in the previous peak of April, 2021. Therefore, since our simulations stops on 2021/10/01, we observe only the start of this wave. Thus the difference between actual and counterfactual vaccination scenarios appears less pronounced.

In Figure 3-A, we investigate what would have happened if the LMIC countries would have been able to start their rollout earlier without changes in allocation volume. We take as a reference point the start of the vaccination campaign in the European Union (EU) which took place, symbolically across all member States, on the 27th of December 2020. It is important to highlight the variance in the real rollout start dates across the countries under study. Indonesia, Bangladesh and Sri Lanka administered the first doses in mid (first country) and late (other two countries) January 2021. Bolivia, Morocco and Ukraine in early, mid and late February respectively. Kenya and Mozambique in early March. Hence, the difference respect to the initial date of the European Union spans between two weeks and three months. Overall the plot shows how an early start would have been beneficial as it would have found a larger fraction of the population susceptible to protect before the Delta wave. However, the magnitude of such effects is heterogeneous in the group of countries. A key factor is the interplay within the amount of vaccine available and the relative shift of the starting time. Sri Lanka and Morocco, that achieved the highest coverage in the group and initiated their campaigns one month later respect to the EU, show around 50% of averted deaths respect to their actual rollout. Only around 30 days can make a big difference. In the case of Kenya and Mozambique the benefits of an early start are more limited but substantial (around 20%). Even with very low vaccination rates a three month head start can make a difference, but its effects are ultimately influenced by the relatively small number of administered vaccine doses. In fact, the percentage of averted deaths is very similar to what we find for Bolivia that has higher vaccination coverage but started only about one month later than the EU. Similarly, the moderate percentage of averted deaths for Indonesia and Bangladesh is due to the small difference between the actual and counterfactual start of the vaccination campaigns.

Finally, we study the extent to which additional NPIs are required in each country to offset the lack of vaccines with respect to high income countries. In this counterfactual we keep the real doses administration as it unfolded in reality. Then, after week 50 of 2020 (a proxy date for the start of the rollout in high income countries), we modify the NPIs making them more restrictive in the countries under study. Since the impact of NPIs is modulated by their strictness and their duration [17, 26–

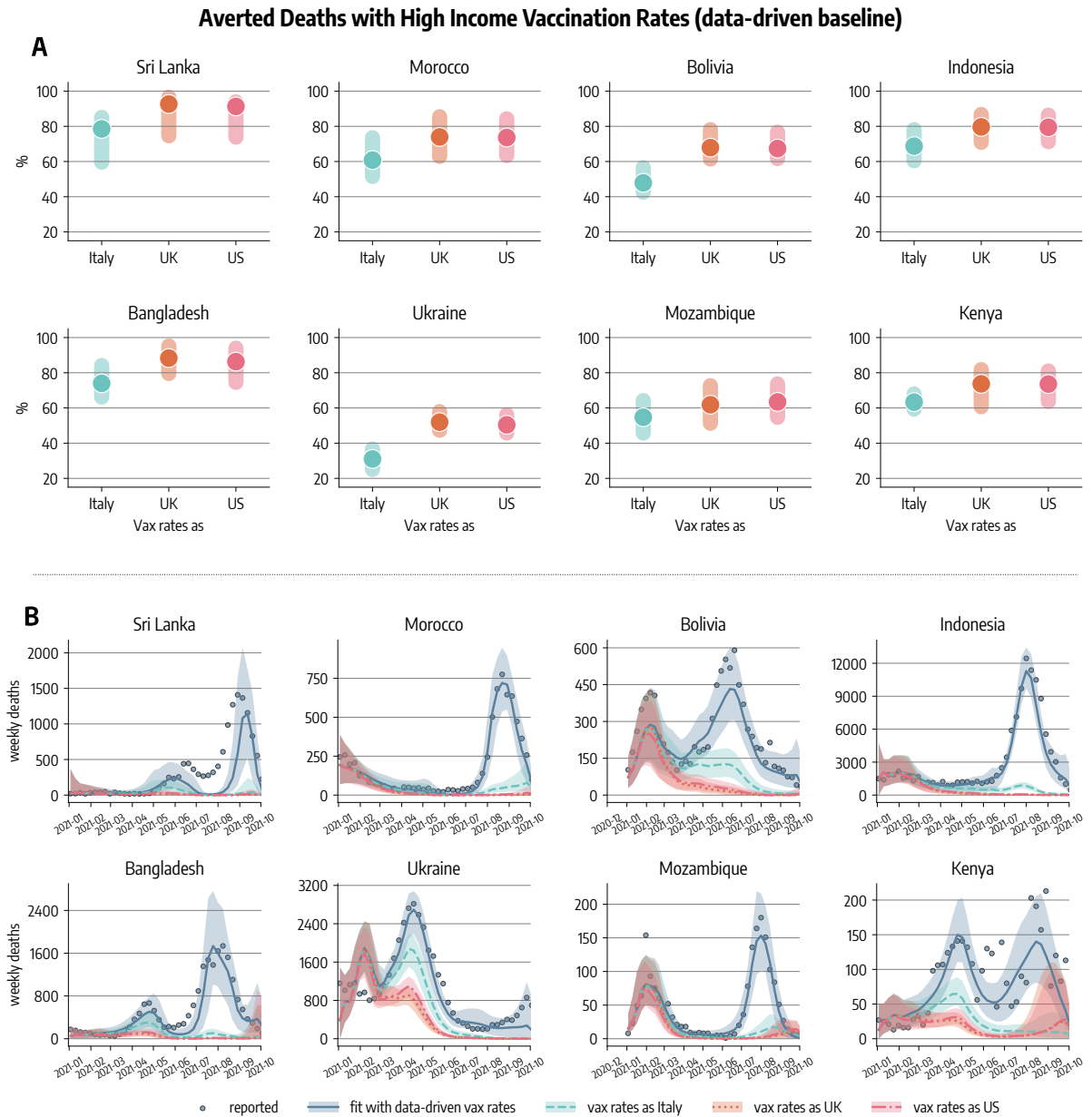


Figure 2: **Counterfactual scenarios - Averted deaths with high-income vaccination rates.** A) Averted deaths (median and 90% CI) expressed as a percentage with respect to the factual vaccination baseline using the vaccination rates of Italy, United Kingdom, and United States. Countries are ordered according to the number of doses actually administered, from highest to lowest. B) Evolution of weekly deaths as reported and as simulated with factual vaccines rates and vaccination rates of Italy, United Kingdom, and United States.

31], we explore a two-dimensional parameter space in which NPIs are $X\%$ stricter with respect to the observed and the tightening of measures is maintained for W weeks. In Figure 3-B, we show the percentage of averted deaths with respect to the real evolution as a function of these two variables. As a comparison, we also show the deaths averted by applying UK vaccination rates as a red dashed contour line (analogous conclusions can be drawn considering Italy and US rates, not shown). In other words, we measure the level of restrictions and their duration necessary to avert the same number of deaths that higher vaccine allocation policies would have been able to. As expected, across the different countries considered, the longer additional NPIs are in place the less strict they need to be in order to avert the same number of deaths. In the case of Indonesia, for example, the level of deaths averted with the UK vaccination rates are matched by either NPIs that are 50% stricter and maintained for 2 months, or by NPIs that are 15% stricter but are maintained for much longer (~ 8 months). More in general, we find that significantly stricter levels of NPIs would be needed in the LMIC countries considered to match the benefits brought by higher vaccine availability. Additionally, we notice that the lower the vaccine coverage in a country, the higher the level of NPIs needed to obtain the same level of averted deaths (see for example Mozambique and Kenya, where little vaccines were delivered respect to Sri Lanka and Morocco). This underlines once again the positive impact of vaccines in LMIC despite the low numbers. It is important to mention how a third variable affects the impact of NPIs: their timing with respect to the prevalence of infections [17, 26–31]. Here, we have fixed their start across all countries analyzed. Hence, such measures are put in place in different epidemiological contexts. For example the end of 2020 in Sri Lanka was far from any pandemic peaks. Instead, in Ukraine, Mozambique and Boliva the end of 2020 was characterized by high prevalence levels that peaked soon after. Hence, the behaviors observed in Figure 3-B are modulated also by the relative timing of the simulated additional NPIs.

Discussion

As of 1st December, 2021, 55% of the global population has received at least one dose of a COVID-19 vaccine. While this is an incredible milestone, vaccines allocation has been characterized by extreme inequality levels. As result, high and upper-middle income countries have vaccination rates that are much higher than LMIC. Their rollout started earlier, and it had a much smaller economic impact (with respect to their GDP and healthcare expenditures). In this context, we studied COVID-19 vaccine inequalities in eight LMIC selected to sample different regions of the world.

We use a computational modeling approach, calibrated to the epidemiological context of each country, to study counterfactual scenarios where each country would have been able to administer vaccines at the same rate as in Italy, the UK, and the US. We estimate that in these counterfactual scenarios the eight countries would have averted more than half (with peaks of 80% and above) of the deaths that actually occurred. We also run a counterfactual scenario where we kept the same number of doses administered in those countries but we assumed an early start of each vaccination campaign. Also in this case we find differences in the impact of an early vaccination campaign start among the eight LMIC, but overall we estimate that a remarkable fraction of death could have been averted by just anticipating the vaccine allocation. Finally, we estimate the strictness of NPIs that each country would have to put in place to offset the lack of vaccines with respect to high-income countries. Across the different LMIC, we find that stronger and sustained NPIs are necessary to obtain a number averted deaths comparable to those estimated in the counterfactual scenarios with higher vaccination rates. This finding, combined with the difficulty of implementing additional NPIs in these settings, underlines once again the largely untapped benefits that vaccines could bring in LMIC.

Our study, as all modeling approaches, comes with limitations. First, the details about the vaccination campaigns may lack detailed or the type of vaccine administered. The compartmental structure used to simulate the disease progression does not capture explicitly asymptomatic transmission as well as different severe outcomes such as hospitalizations and ICUs admissions. The model operates at national level thus neglecting geographical heterogeneities that could reveal yet other layers of inequalities, within each country. Although we consider variable IFRs across countries we do not explicitly account for comorbidities nor limited healthcare access. Finally, it is worth remarking that the counterfactual scenarios do not take into account vaccine hesitancy, nor the cost of the supply chain necessary to receive, store, distribute and administer doses.

Overall the picture emerging from our analysis shows that vaccine inequality, in both the number of doses available and the timeline of delivery, drastically reduced the impact of vaccination campaigns in the sample of LMIC studied. As the world is facing the Omicron variant of concern (which appears to have a relative advantage with respect to Delta and larger immune escape capabilities) [32], countries

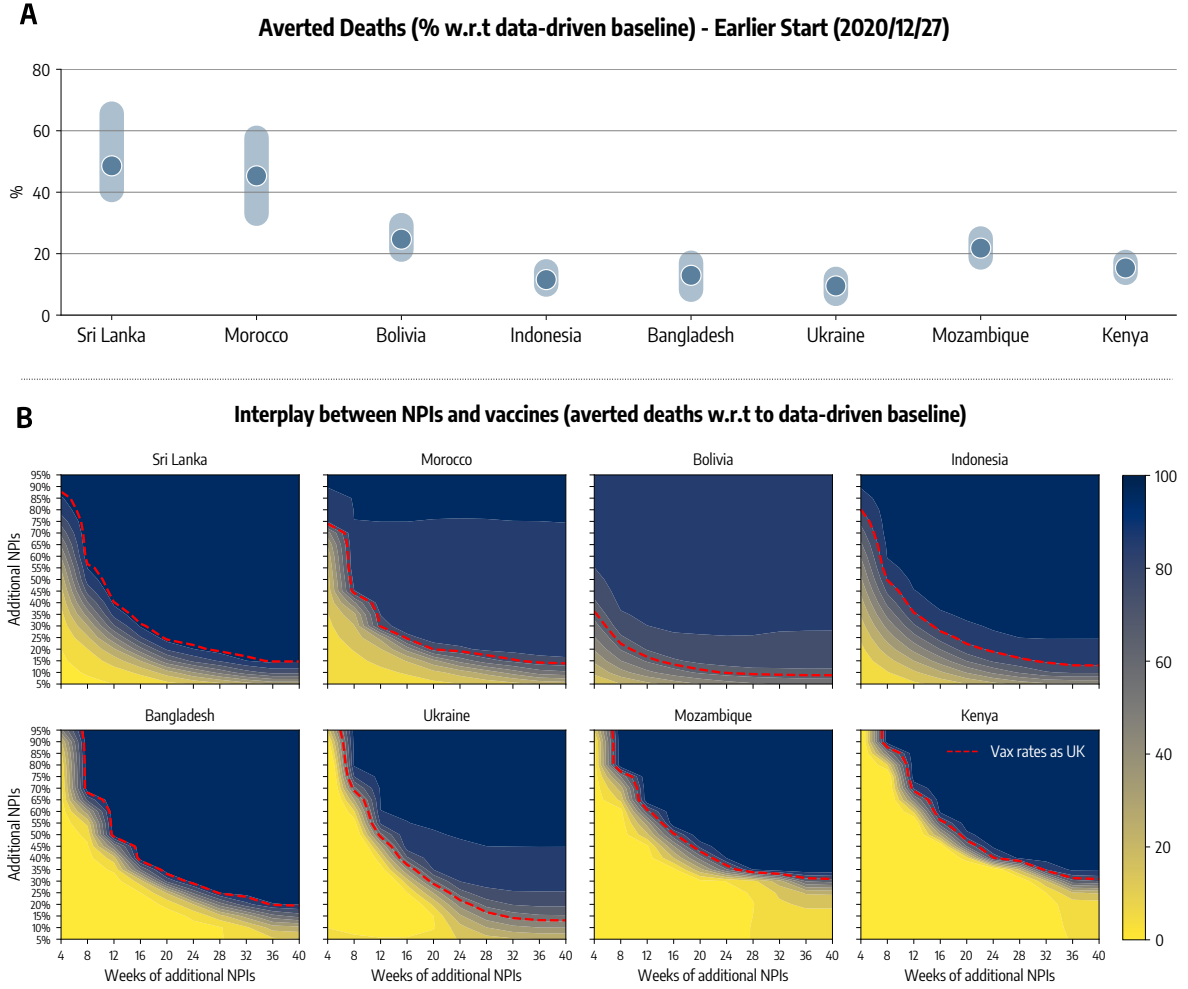


Figure 3: **Counterfactual scenarios - Earlier start and the role of NPIs.** A) Averted deaths (median and 90% CI) with respect to the factual vaccination baseline anticipating the start of vaccination campaigns to 2020/12/27. B) Contourplot of averted deaths (median %) with respect to simulations with factual vaccines in the case of additional NPIs. We explore both more strict and sustained NPIs. Percentage of averted deaths in the case of vaccination rate as the UK is reported as reference (red dashed line).

are rushing to progress their vaccination rollouts, which now include also booster shots. In many of these countries, there have been more boosters than first doses in several LMIC. Furthermore, many of these countries are facing vaccine hesitancy challenges that effectively make a sizable fraction of vaccine doses unutilized. Potentially a staggering number of vaccines doses are currently not used and as much as 1B might be disposed due to expiration dates by end of 2021 [33]. Vaccine inequality will persist to be a critical issue in the mitigation and control worldwide of the COVID-19 pandemic. The presented approach is potentially relevant in defining strategies aimed at minimizing the effect of inequalities in vaccine allocation across countries.

Acknowledgements

This work was partially supported by the Bill & Melinda Gates Foundation (award number INV006010). We acknowledge support from Google Cloud and Google Cloud Research Credits program. The content is solely the responsibility of the authors. All authors thank the High Performance Computing facilities at Greenwich University. N.G. acknowledges support from the Doctoral Training Alliance.

References

- [1] Ezekiel J Emanuel, Govind Persad, Adam Kern, Allen Buchanan, Cécile Fabre, Daniel Halliday, Joseph Heath, Lisa Herzog, RJ Leland, Ephrem T Lemango, et al. An ethical framework for global vaccine allocation. *Science*, 369(6509):1309–1312, 2020.
- [2] Caroline E. Wagner, Chadi M. Saad-Roy, Sinead E. Morris, Rachel E. Baker, Michael J. Mina, Jeremy Farrar, Edward C. Holmes, Oliver G. Pybus, Andrea L. Graham, Ezekiel J. Emanuel, Simon A. Levin, C. Jessica E. Metcalf, and Bryan T. Grenfell. Vaccine nationalism and the dynamics and control of sars-cov-2. *Science*, 373(6562):eabj7364, 2021.
- [3] Caroline Buckee, Abdisalan Noor, and Lisa Sattenspiel. Thinking clearly about social aspects of infectious disease transmission. *Nature*, 595(7866):205–213, 2021.
- [4] Richard L Oehler and Vivian R Vega. Conquering covid: How global vaccine inequality risks prolonging the pandemic. In *Open Forum Infectious Diseases*, volume 8, page ofab443. Oxford University Press US, 2021.
- [5] Nicolò Gozzi, Michele Tizzoni, Matteo Chinazzi, Leo Ferres, Alessandro Vespignani, and Nicola Perra. Estimating the effect of social inequalities on the mitigation of COVID-19 across communities in Santiago de Chile. *Nature Communications*, 12(1):2429, 2021.
- [6] Giulia Pullano, Eugenio Valdano, Nicola Scarpa, Stefania Rubrichi, and Vittoria Colizza. Evaluating the effect of demographic factors, socioeconomic factors, and risk aversion on mobility during the covid-19 epidemic in france under lockdown: a population-based study. *The Lancet Digital Health*, 2(12):e638–e649, 2020.
- [7] Giovanni Bonaccorsi, Francesco Pierri, Matteo Cinelli, Andrea Flori, Alessandro Galeazzi, Francesco Porcelli, Ana Lucia Schmidt, Carlo Michele Valensise, Antonio Scala, Walter Quattrocioni, and Fabio Pammolli. Economic and social consequences of human mobility restrictions under covid-19. *Proc Natl Acad Sci USA*, 117(27):15530–15535, jun 2020.
- [8] Joakim A. Weill, Matthieu Stigler, Olivier Deschenes, and Michael R. Springborn. Social distancing responses to covid-19 emergency declarations strongly differentiated by income. *Proc Natl Acad Sci USA*, 117(33):19658–19660, jul 2020.
- [9] Samuel P Fraiberger, Pablo Astudillo, Lorenzo Candeago, Alex ChUNET, Nicholas KW Jones, Maham Faisal Khan, Bruno Lepri, Nancy Lozano Gracia, Lorenzo Lucchini, Emanuele Massaro, et al. Uncovering socioeconomic gaps in mobility reduction during the covid-19 pandemic using location data. *arXiv preprint arXiv:2006.15195*, 2020.
- [10] Gonzalo E Mena, Pamela P Martinez, Ayesha S Mahmud, Pablo A Marquet, Caroline O Buckee, and Mauricio Santillana. Socioeconomic status determines covid-19 incidence and related mortality in santiago, chile. *Science*, 372(6545), 2021.

- [11] Won Do Lee, Matthias Qian, and Tim Schwanen. The association between socioeconomic status and mobility reductions in the early stage of england’s covid-19 epidemic. *Health & Place*, 69:102563–102563, 2021.
- [12] Serina Chang, Emma Pierson, Pang Wei Koh, Jaline Gerardin, Beth Redbird, David Grusky, and Jure Leskovec. Mobility network models of COVID-19 explain inequities and inform reopening.
- [13] Eugenio Valdano, Jonggul Lee, Shweta Bansal, Stefania Rubrichi, and Vittoria Colizza. Highlighting socio-economic constraints on mobility reductions during covid-19 restrictions in france can inform effective and equitable pandemic response. *Journal of travel medicine*, 28(4):taab045, 2021.
- [14] Global Dashbord for Vaccine Equity. <https://data.undp.org/vaccine-equity/>, 2021. Accessed: 2021-11-30.
- [15] Mikael Sunnåker, Alberto Giovanni Busetto, Elina Numminen, Jukka Corander, Matthieu Foll, and Christophe Dessimoz. Approximate bayesian computation. *PLOS Computational Biology*, 9(1):1–10, 01 2013.
- [16] Amanda Minter and Renata Retkute. Approximate bayesian computation for infectious disease modelling. *Epidemics*, 29:100368, 2019.
- [17] Nicola Perra. Non-pharmaceutical interventions during the covid-19 pandemic: A review. *Physics Reports*, 2021.
- [18] Valentina Marziano, Giorgio Guzzetta, Alessia Mammone, Flavia Riccardo, Piero Poletti, Filippo Trentini, Mattia Manica, Andrea Siddu, Antonino Bella, Paola Stefanelli, et al. The effect of covid-19 vaccination in italy and perspectives for living with the virus. *Nature communications*, 12(1):1–8, 2021.
- [19] Nicolò Gozzi, Matteo Chinazzi, Jessica T. Davis, Kunpeng Mu, Ana Pastore y Piontti, Marco Ajelli, Nicola Perra, and Alessandro Vespignani. Anatomy of the first six months of covid-19 vaccination campaign in italy. *medRxiv*, 2021.
- [20] Coronavirus (covid-19) vaccinations. <https://ourworldindata.org/covid-vaccinations>, 2020. Accessed: 2020-11-30.
- [21] J. Klugman. Human development report 2010 – 20th anniversary edition. the real wealth of nations: Pathways to human development. 2010.
- [22] Robert Verity, Lucy Okell, Ilaria Dorigatti, Peter Winskill, Charles Whittaker, Natsuko Imai, Gina Cuomo-Dannenburg, Hayley Thompson, Patrick Walker, Han Fu, Amy Dighe, Jamie Griffin, Marc Baguelin, Sangeeta Bhatia, Adhiratha Boonyasiri, Anne Cori, Zulma M. Cucunubá, Rich FitzJohn, Katy Gaythorpe, and Neil Ferguson. Estimates of the severity of coronavirus disease 2019: a model-based analysis. *The Lancet Infectious Diseases*, 20, 03 2020.
- [23] Laura Matrajt, Julia Eaton, Tiffany Leung, Dobromir Dimitrov, Joshua T Schiffer, David A Swan, and Holly Janes. Optimizing vaccine allocation for COVID-19 vaccines shows the potential role of single-dose vaccination. *Nature Communications*, 12(1):3449, 2021.
- [24] Laura Matrajt, Julia Eaton, Tiffany Leung, and Elizabeth R. Brown. Vaccine optimization for covid-19: Who to vaccinate first? *Science Advances*, 7(6), 2020.
- [25] Nicolò Gozzi, Matteo Chinazzi, Jessica T Davis, Kunpeng Mu, Ana Pastore y Piontti, Marco Ajelli, Nicola Perra, and Alessandro Vespignani. Estimating the spreading and dominance of sars-cov-2 voc 202012/01 (lineage b. 1.1. 7) across europe. *medRxiv*, 2021.
- [26] Jessica T Davis, Matteo Chinazzi, Nicola Perra, Kunpeng Mu, Ana Pastore y Piontti, Marco Ajelli, Natalie E Dean, Corrado Gioannini, Maria Litvinova, Stefano Merler, et al. Cryptic transmission of sars-cov-2 and the first covid-19 wave. *Nature*, 600(7887):127–132, 2021.
- [27] Nils Haug, Lukas Geyrhofer, Alessandro Londei, Elma Dervic, Amélie Desvars-Larrive, Vittorio Loreto, Beate Pinior, Stefan Thurner, and Peter Klimek. Ranking the effectiveness of worldwide covid-19 government interventions. *Nature human behaviour*, 4(12):1303–1312, 2020.

- [28] Easton R White and Laurent Hébert-Dufresne. State-level variation of initial covid-19 dynamics in the united states. *PloS one*, 15(10):e0240648, 2020.
- [29] Sheikh Taslim Ali, Lin Wang, Eric HY Lau, Xiao-Ke Xu, Zhanwei Du, Ye Wu, Gabriel M Leung, and Benjamin J Cowling. Serial interval of sars-cov-2 was shortened over time by nonpharmaceutical interventions. *Science*, 369(6507):1106–1109, 2020.
- [30] Sarah Jefferies, Nigel French, Charlotte Gilkison, Giles Graham, Virginia Hope, Jonathan Marshall, Caroline McElnay, Andrea McNeill, Petra Muellner, Shevaun Paine, et al. Covid-19 in new zealand and the impact of the national response: a descriptive epidemiological study. *The Lancet Public Health*, 5(11):e612–e623, 2020.
- [31] Nazrul Islam, Stephen J Sharp, Gerardo Chowell, Sharmin Shabnam, Ichiro Kawachi, Ben Lacey, Joseph M Massaro, Ralph B D’Agostino, and Martin White. Physical distancing interventions and incidence of coronavirus disease 2019: natural experiment in 149 countries. *bmj*, 370, 2020.
- [32] Juliet R.C. Pulliam, Cari van Schalkwyk, Nevashan Govender, Anne von Gottberg, Cheryl Cohen, Michelle J. Groome, Jonathan Dushoff, Koleka Mlisana, and Harry Moultrie. Increased risk of sars-cov-2 reinfection associated with emergence of the omicron variant in south africa. *medRxiv*, 2021.
- [33] More Than A Billion Available Stock Of Western COVID-19 Vaccines By The End Of 2021. <https://www.airfinity.com/insights/more-than-a-billion-available-stock-of-western-covid-19-vaccines-by-the-end>, 2021.

Supplementary Material for *Estimating the impact of COVID-19 vaccines allocation inequalities: a modeling study*

Nicolò Gozzi¹, Matteo Chinazzi², Nicola Perra^{1,2}, Alessandro Vespignani²

¹ Networks and Urban Systems Centre, University of Greenwich, UK

² Laboratory for the Modeling of Biological and Socio-technical Systems, Northeastern University, Boston, MA USA

January 16, 2022

Contents

1	Data	2
2	Epidemic model	2
3	Model calibration	2
4	Non-pharmaceutical interventions	5
5	Counterfactual scenarios	5
5.1	Vaccination rates of high income countries	5
5.2	Earlier start of actual vaccinations	5
5.3	Additional NPIs	5
6	Estimating the impact of the factual vaccination campaigns	7
7	Averted deaths - Counterfactual scenarios	9

1 Data

Data about demographics comes from the United Nation World Population Prospects [1]. Epidemiological data are taken from the COVID-19 Data Repository by the Center for Systems Science and Engineering (CSSE) at Johns Hopkins University and from official sources [2]. Data about vaccination are taken from the United Nations Development Programme via their Global Futures Platform [3] and from Our World in Data [4].

2 Epidemic model

We adopt a SLIR-like compartmental model (see Figure 1 for a schematic depiction). The susceptible individuals are placed in the compartment S . Getting in contact with the Infectious (I) they transition to the compartment of the Latent (L). Latent individuals are infected but become infectious only after ϵ^{-1} days when they eventually pass to the compartment I . After μ^{-1} days, infectious subjects finally transition to the compartment of the Recovered (R). By considering the COVID-19 characteristics we set $\epsilon^{-1} = 4days$ and $\mu^{-1} = 2.5days$. [5, 6]. Individuals are divided into 10 age groups (0–9, 10–19, 20–24, 25–29, 30–39, 40–49, 50–59, 60–69, 70–79, 80+). The age-stratified rate of interaction are defined by the country specific contacts matrix C from Ref. [7]. We compute the number of deaths on daily recovered using as basis (see more information below) the age-stratified Infection Fatality Rate (IFR) from Ref. [8]. To account for possible delays due to hospitalization and reporting between the transition $I \rightarrow R$ and actual death we record the number of deaths computed on the recovered of day t only after Δ days. We also introduce a seasonal term to capture modulation of the force of infection regulated by changes in factors such as temperature and humidity [9, 10]. This means that in our simulation R_t is multiplied by a rescaling factor $s_i(t)$ defined as $s_i(t) = \frac{1}{2} \left[\left(1 - \frac{\alpha_{min}}{\alpha_{max}} \right) \sin \left(\frac{2\pi}{365} (t - t_{max,i}) + \frac{\pi}{2} \right) + 1 + \frac{\alpha_{min}}{\alpha_{max}} \right]$, where i refers to the hemisphere considered, and $t_{max,i}$ is the day associated to the maximum of the rescaling function. For the northern hemisphere it is set to January 15th and to July 15th for the southern hemisphere, while we consider no seasonal modulation in the tropical hemisphere. If a country extends across multiple zones, the seasonal factor is a weighted average of the different $s_i(t)$ according to the population living in the different hemispheres. We fix $\alpha_{max} = 1$ and consider α_{min} as a free parameter (see more details below).

On top of this disease dynamics we model both vaccinations and the introduction of a second, more transmissible virus strain. Individuals that received a single dose of vaccines are placed in the V_1 compartment. For these individuals the force of infection is reduced by a factor $(1 - VE_{S1})$. Additionally, also the IFR of V_1 is reduced by a factor of $(1 - VE_{M1})$. It follows that, in our simulations, the overall efficacy of a single dose of vaccine against death is $VE_1 = 1 - (1 - VE_{S1})(1 - VE_{M1})$. After receiving the second dose, V_1 individuals transition to V_2 compartment. Similarly, force of infection and IFR of V_2 is reduced, respectively, by $(1 - VE_{S2})$ and $(1 - VE_{M2})$, implying an overall efficacy of $VE_2 = 1 - (1 - VE_{S2})(1 - VE_{M2})$. We also assume that vaccinated individuals are less infectious by a factor $(1 - VE_I)$ [11]. We assume that S , L , and R individuals can receive the vaccines and that the rollout proceeds prioritizing the elderly. This means that, in our model, vaccines are distributed in decreasing age order until all 50+ individuals are vaccinated, after vaccines are distributed homogeneously to the age groups 10–50. We inform the model with the number of daily 1st and 2nd doses in different countries from Ref. [12]. In this work we set $VE_1 = 80\%$ ($VE_{S1} = 70\%$), $VE_2 = 90\%$ ($VE_{S2} = 80\%$), and $VE_I = 40\%$ [11]. Since the effect of vaccines is not immediate, we introduce a delay of $\Delta_V = 14days$ between administration and vaccine protection.

We add specific L and I compartments to account for the introduction and emergence of the more transmissible SARS-CoV-2 variant of concern Delta. Looking at genomic sequence data from Ref. [13–15] we get a proxy date for its introduction (more details provided below). We imagine that Delta is ψ times more transmissible than the strain circulating previously and has a shorter latent period $\epsilon_{Delta}^{-1} = 3days$ [16]. We also assume that vaccines have a reduced efficacy against Delta VOC: $VE_1^{Delta} = 70\%$ ($VE_{S1}^{Delta} = 30\%$), $VE_2^{Delta} = 90\%$ ($VE_{S2}^{Delta} = 60\%$) [11].

3 Model calibration

The free parameters of the model are calibrated through a rejection algorithm based on Approximate Bayesian Computation [17, 18]. We define a prior distribution $P(\theta)$ on the free parameters θ . At each step of the iterative algorithm, we sample a set of parameters $\hat{\theta}$ from $P(\theta)$ and an instance of the model

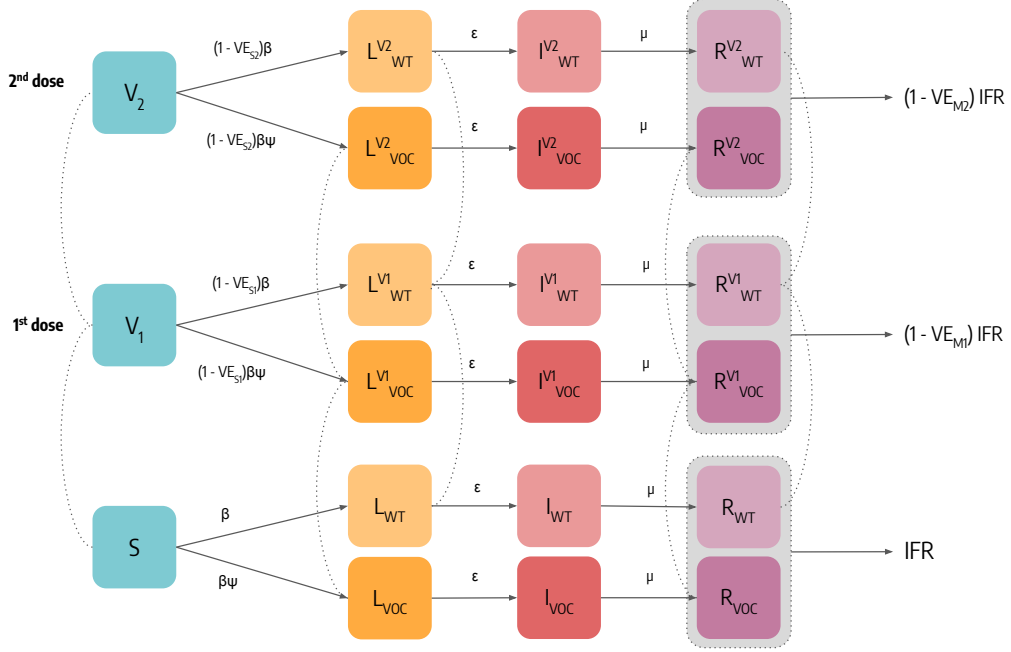


Figure 1: **Epidemic Model.**

is generated using $\hat{\theta}$. Then, an output quantity of the model E' is compared to the corresponding real quantity E using an error metric $S(E, E')$: if $S(E, E')$ is smaller than a tolerance δ , $\hat{\theta}$ is accepted otherwise is rejected. Repeating this procedure iteratively we obtain an approximation of the posterior distribution of the parameters θ . In this work we consider weekly deaths as output quantity and the weighted mean absolute percentage error (wMAPE) as distance metric. The free parameters and the relative priors are:

- the transmission rate β ; we explore uniformly values such that the R_t on the first simulation date is between 0.6 and 2.0;
- the delay in deaths $\Delta \sim U(10, 35)$ [19];
- the seasonality parameter $\alpha_{min} \sim U(0.5, 1.0)$ (0.5 indicates strong seasonality while 1.0 absence of seasonality);
- the percentage of deaths reported $\sim U(5\%, 100\%)$;
- the initial number of infected individuals; we explore uniformly values between 1 and 20 times the number of cases notified in the 7 days prior the beginning of the simulation (Inf_{start}^{mult}). We divide these individuals in the infected compartments (L, I) proportionally to the time spent there by individuals (ϵ^{-1} for L and μ^{-1} for I);
- the initial number of recovered; we explore uniformly values between 1 and 20 times the total number of reported cases up to the start of the simulation (Rec_{start}^{mult});
- the relative transmissibility advantage of the Delta VOC $\psi \sim U(1.0, 2.5)$
- the date of the introduction of the Delta VOC. We consider values between 1 month before and after the date when Delta was responsible for at least 5% of sequenced samples according to the data from Ref. [13–15]. If genomics data are not available, we consider data from neighboring proxy countries;
- the IFR multiplier $\sim U(0.5, 2.0)$.

The model is calibrated separately for each country during the period 2020/12/01 – 2021/10/01. In Tab. 1 and Tab. 2 we report the posterior distributions (median and interquartile range) of the free parameters.

	Sri Lanka	Morocco	Bolivia	Indonesia
R_t^{start}	0.88 [0.86, 0.91]	1.1 [1.09, 1.17]	1.33 [1.26, 1.41]	1.26 [1.22, 1.3]
Δ	21.0 [19.0, 26.0]	15.0 [12.0, 20.0]	22.0 [19.0, 27.0]	28.0 [25.0, 30.0]
α_{min}	0.7 [0.69, 0.73]	0.7 [0.56, 0.96]	0.66 [0.56, 0.77]	0.72 [0.66, 0.91]
Inf_{start}^{mult}	8.11 [2.63, 17.34]	6.61 [4.01, 12.04]	13.2 [8.88, 16.73]	18.59 [11.2, 29.41]
Rec_{start}^{mult}	32.75 [6.0, 41.66]	10.78 [7.4, 12.75]	15.54 [13.45, 19.93]	34.88 [14.85, 42.28]
<i>Date intro. VOC</i>	04/23 [04/20, 04/25]	04/13 [04/04, 04/27]	07/26 [07/04, 08/04]	04/17 [04/12, 05/03]
% deaths reported	55.0 [35.0, 76.0]	39.0 [28.0, 56.0]	88.0 [80.0, 95.0]	73.0 [58.0, 87.0]
<i>IFR Multiplier</i>	1.24 [0.84, 1.62]	1.02 [0.72, 1.42]	1.74 [1.58, 1.88]	1.46 [1.14, 1.72]
ψ	2.43 [2.23, 2.46]	1.81 [1.73, 2.16]	1.31 [1.17, 1.43]	1.41 [1.36, 1.53]

Table 1: **Posterior distributions of free parameters obtained via ABC calibration (Sri Lanka, Morocco, Bolivia, Indonesia).** We show median and interquartile range of the different parameters. Dates are represented with a *mm – dd* format and refer all to the year 2021.

	Bangladesh	Ukraine	Mozambique	Kenya
R_t^{start}	1.13 [1.09, 1.19]	1.57 [1.51, 1.65]	1.57 [1.5, 1.6]	1.38 [1.36, 1.43]
Δ	19.0 [16.0, 26.0]	29.0 [29.0, 32.0]	29.0 [24.0, 31.0]	27.0 [25.0, 31.0]
α_{min}	0.68 [0.58, 0.8]	0.69 [0.65, 0.85]	0.71 [0.6, 0.87]	0.68 [0.6, 0.82]
Inf_{start}^{mult}	11.66 [7.55, 19.67]	1.2 [1.1, 1.29]	28.57 [20.6, 34.83]	27.78 [18.5, 34.87]
Rec_{start}^{mult}	27.49 [22.06, 35.27]	3.46 [3.35, 4.06]	30.09 [16.78, 37.06]	29.77 [17.65, 37.51]
<i>Date intro. VOC</i>	04/09 [03/24, 05/03]	05/18 [05/10, 05/31]	04/10 [03/28, 04/22]	04/19 [04/03, 05/04]
% deaths reported	15.5 [11.0, 23.0]	61.0 [45.0, 78.0]	5.0 [4.0, 8.0]	7.0 [5.0, 11.0]
<i>IFR Multiplier</i>	0.98 [0.7, 1.4]	1.24 [0.92, 1.56]	0.98 [0.7, 1.4]	0.98 [0.7, 1.4]
ψ	1.8 [1.65, 1.98]	1.52 [1.36, 1.67]	1.34 [1.24, 1.47]	1.27 [1.11, 1.41]

Table 2: **Posterior distributions of free parameters obtained via ABC calibration (Bangladesh, Ukraine, Mozambique, Kenya).** We show median and interquartile range of the different parameters. Dates are represented with a *mm – dd* format and refer all to the year 2021.

4 Non-pharmaceutical interventions

We model the effects of non-pharmaceutical interventions on contacts using the COVID-19 Community Mobility Report By Google [20]. The dataset provides, for various countries and spatial resolutions, a percentage change in mobility $r(t)$ on day t . We convert this quantity into a contacts reduction parameters $c(t)$ following the relation: $c(t) = (1 + r(t)/100)^2$. Indeed, the number of contacts scale with the square of the number of individuals. For example, a percentage reduction of -20% translates into a contacts reduction factor of 0.64. In the simulations the contacts matrix C is multiplied by this reduction parameter $c(t)$ to account for the modulation in contacts induced by NPIs. The dataset provides mobility changes with respect to specific locations. In this work, we compute $r(t)$ we use the average of the fields `workplaces percent change from baseline`, `retail and recreation percent change from baseline` and `transit stations percent change from baseline`.

5 Counterfactual scenarios

We studied three counterfactual scenarios.

5.1 Vaccination rates of high income countries

We propose scenarios in which the eight LMIC considered manage the same vaccines availability of three high income countries: Italy, United Kingdom, and United States. To do so, we simply run simulations in which, instead of the actual vaccination data of the LMIC considered, we use the daily number of first and second doses administered in the three high income countries. To account for different population sizes among countries, we rescale the number of doses available in the counterfactual. For example, consider the case when we apply to Mozambique the vaccination rates of Italy. If Italy administered X_t^{Italy} doses on day t , in the counterfactual scenario we administer $X_t^{Mozambique} = X_t^{Italy} \frac{N_{Mozambique}}{N_{Italy}}$. In Fig. 2 we show the cumulative number of doses given per 100 in these counterfactual vaccination scenarios with respect to the data-driven case.

5.2 Earlier start of actual vaccinations

As a second counterfactual analysis, we anticipate the actual vaccination campaign in the eight LMIC in order to match the start of vaccine rollout in high income countries. As new starting date we choose the 2020/12/27, when COVID-19 vaccinations started in most of European Union countries [21]. If the shift of vaccination data causes missing data at the end of the time series, we fill it considering the average number of doses administered during the last 7 days.

5.3 Additional NPIs

We consider simulations in which we modify the actual NPIs quantified with the COVID-19 Community Mobility Report. More in detail, given the contacts reduction factor of week t $c(t)$, in the new simulations with $X\%$ additional NPIs the new factor will be $c'(t) = c(t)(1 - X/100)$. The additional level of NPIs is applied to contacts reduction factors after week 50 of 2020, a proxy date for the start of vaccinations in the high income countries considered (Italy, UK, and US). Indeed, our goal is to estimate the additional amount of NPIs needed to match the number of deaths averted when applying vaccination rates of these countries. Finally, the tightening of NPIs is sustained for a limited number of weeks. We explore multiple scenarios with NPIs that are from 5% to 95% tougher and that are sustained for a number of weeks between 4 and 40. In practice, we run additional simulations in which we modify the NPIs as just described and we compute the fraction of averted deaths with respect to simulations with actual NPIs and vaccine rollout.

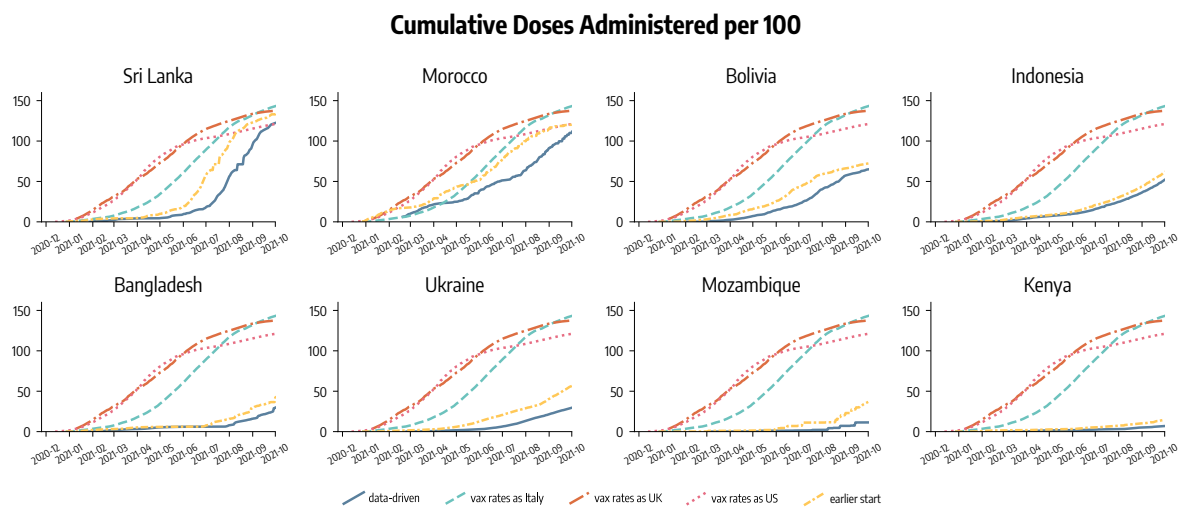


Figure 2: Cumulative number of doses given per 100 in different scenarios.

6 Estimating the impact of the factual vaccination campaigns

In Figure 3-A we plot the evolution of the percentage of partially and fully vaccinated in the eight countries up to 2021/10/01. As clear from the graphs, there is a high level of heterogeneity. We go from fractions of fully vaccinated above 50% in Sri Lanka to values below 10% in Kenya and Mozambique. Indonesia and Bolivia are around the middle between these two groups with a fraction of fully vaccinated close to 20%. When interpreting the numbers it is important to recognize the differences in terms of populations. Indonesia and Bangladesh are the largest with 273M and 165M people respectively. Sri Lanka and Bolivia are the smallest with 21M and 11M residents respectively. Hence, the differences in terms of the absolute number of vaccinated individuals and doses administered span several orders of magnitudes among these countries.

In Figure 3-B, we show the real data of confirmed deaths (dark blue dots). In all countries, the latest epidemic wave, caused by the Delta variant, was, unfortunately, the most deadly. Clearly in contrast with observations across high income countries where, despite the increased transmissibility and severity, the Delta wave was strongly limited by high vaccination rates with respect to the previous [22, 23]. This observation is a first clear hint about the impact that vaccines could have had in these settings. In the plots, we also report the median and confidence intervals of our fits (light green lines and shaded areas). Across the board, the model can capture the evolution of the pandemic with accuracy. It is however important to highlight the few misses. In the case of Sri Lanka the model produces a peak that is slightly delayed with respect to observations. In the case of Ukraine, the models' median trend does not capture the latest increase of deaths, though the real data is still within confidence intervals. Each plot reports also the model's prediction of what would have happened in absence of vaccines (red dashed lines and shaded areas). In particular, we run the model keeping all the same fitted parameters, NPIs, but remove all doses administered. In doing so, we provide estimates of the impact of the actual vaccines in each country. Again, we find large heterogeneity induced by the radically different vaccination coverage. Countries that managed to vaccinate more, such as Morocco and Sri Lanka, show the largest differences between the real evolution of confirmed deaths and those in the hypothetical scenario without vaccines (i.e., baseline). Conversely, in countries such as Kenya, and Mozambique, that have a minimal vaccination coverage, the differences are very small and barely visible. In Figure 3-C, we plot the averted deaths thanks to the vaccination rollout with respect to the baseline without vaccines. While interpreting the results and comparing countries it is important to stress how the model is fitted separately to each nation. Hence, some values of the free parameters such as the transmissibility of the strains circulating might be estimated as slightly different even though they refer to the same variants. For example, the posterior distribution for the relative transmissibility advantage of the Delta variant with respect to Alpha peaks at 1.8 in Morocco while at 2.4 in Sri Lanka. These are effective parameters selected based on the available data. As such, they factor in many behavioral factors that are not explicitly modeled. Examples are the relations among mobility reduction, contact rates modifications, and infections. These might differ in different contexts/environments and affect the scenarios modelled here. The plot confirms the picture emerging from panel B but provides a more clear estimation of the impact of vaccines. Namely, in Sri Lanka and Morocco, the vaccine rollout averted about 70% of the deaths with respect to the baseline. In Bolivia, Indonesia, and Bangladesh the numbers are lower but still significant. Finally, in the case of Ukraine, Kenya, and Mozambique the doses administered are very limited but their impact is still positive. For Ukraine, we note that the confidence intervals show how the impact of vaccines cannot be fully discerned from stochastic effects (see the negative values). It is important to stress this point. The plot does not suggest that the country would have been better off without vaccines. However, the number of doses administered is small and their impact in some simulations is close to the stochastic effects.

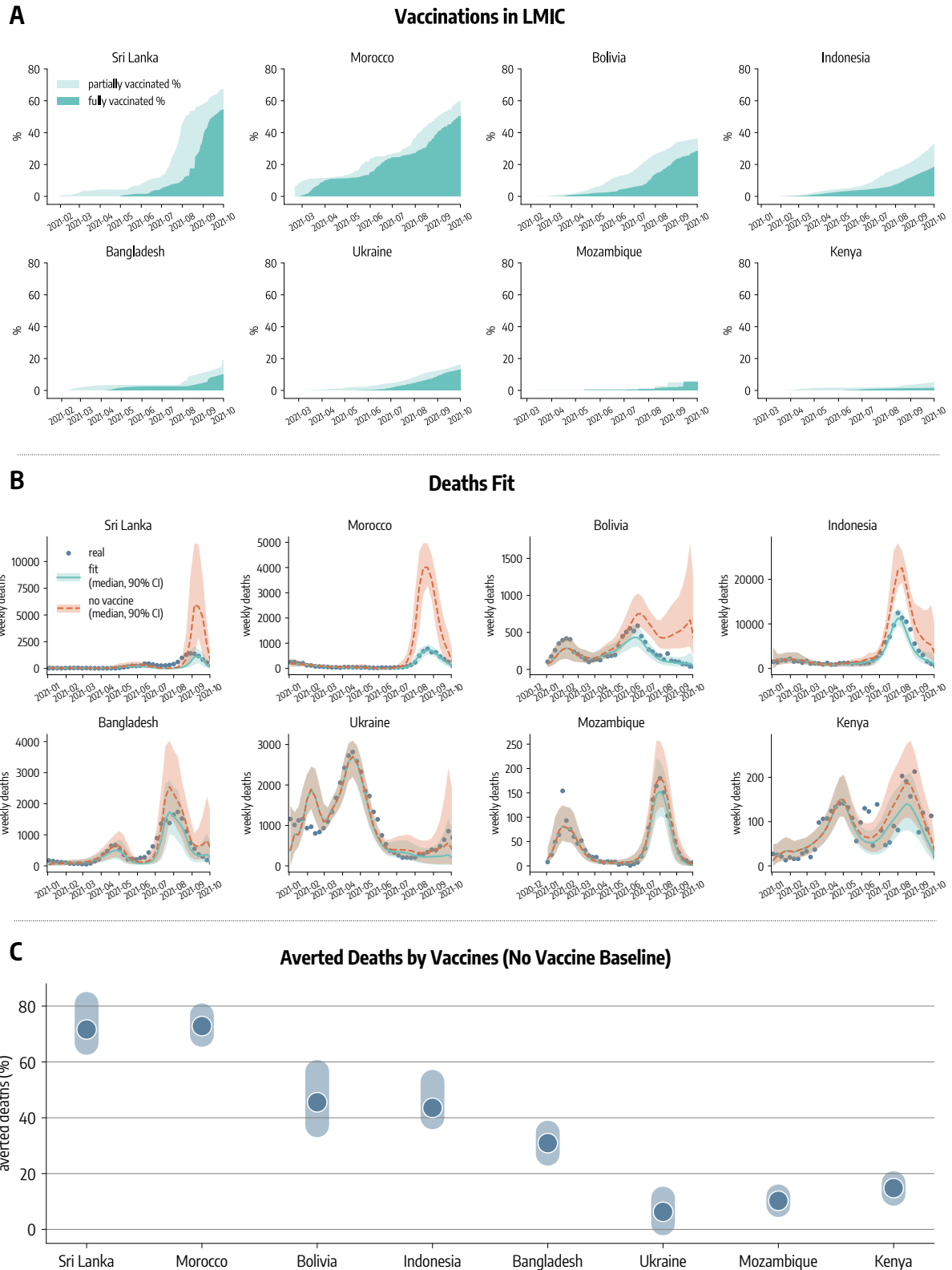


Figure 3: **Vaccination campaign and its effect.** A) Evolution in time of percentage of fully and partially vaccinated individuals in different countries. B) Weekly deaths as reported, as simulated by our model with data-driven vaccines administration, and as simulated by our model without vaccines administered. C) Estimated percentage (median and 90% CI) of deaths averted by vaccines with respect to the baseline simulations without vaccines.

7 Averted deaths - Counterfactual scenarios

In Tab. 3 and Tab. 4 are reported for the different countries considered the number of deaths avoided in the counterfactual scenarios with respect to simulations with data-driven vaccine rollouts. More in detail, Tab. 3 shows the number of averted deaths without accounting for underreporting. On the other hand, the figures reported Tab. 4 take into account the biases of reporting estimated via the ABC procedure. Therefore, the numbers reported in Tab. 4 represent the real estimated number of potentially averted deaths in counterfactual scenarios.

Averted Deaths - Counterfactual Scenarios (data-driven baseline, without underreporting)				
	Vax rates as Italy	Vax rates as UK	Vax rates as US	Earlier Start (2020/12/27)
<i>Sri Lanka</i>	5,546 [3,597 - 7,197]	6,536 [4,188 - 8,427]	6,403 [4,168 - 8,253]	3,641 [2,404 - 5,199]
<i>Morocco</i>	4,352 [3,360 - 5,210]	5,192 [4,297 - 6,101]	5,178 [4,274 - 6,097]	3,217 [2,186 - 4,172]
<i>Bolivia</i>	4,196 [3,540 - 5,134]	5,965 [5,068 - 7,064]	5,909 [5,052 - 6,975]	2,156 [1,781 - 2,605]
<i>Indonesia</i>	76,768 [66,880 - 92,002]	89,371 [76,820 - 105,293]	89,341 [77,179 - 105,120]	13,041 [10,771 - 16,213]
<i>Bangladesh</i>	12,964 [9,760 - 17,560]	15,202 [11,575 - 20,281]	14,944 [11,243 - 19,977]	2,177 [1,289 - 3,301]
<i>Ukraine</i>	12,342 [9,092 - 15,887]	20,851 [17,048 - 24,971]	20,239 [16,498 - 24,307]	3,789 [2,547 - 5,158]
<i>Mozambique</i>	927 [683 - 1,220]	1,048 [761 - 1,377]	1,085 [807 - 1,409]	373 [286 - 473]
<i>Kenya</i>	1,945 [1,517 - 2,410]	2,234 [1,604 - 2,868]	2,245 [1,663 - 2,848]	471 [367 - 582]

Table 3: Number of deaths averted with vaccination rates of high income countries (Italy, UK, US) and with earlier start of vaccination campaign (2020/12/27). The baseline are simulations with actual, data-driven vaccine rollouts. Median and 90% CI are reported. These figures do account for underreporting of deaths.

Averted Deaths - Counterfactual Scenarios (data-driven baseline, with underreporting)				
	Vax rates as Italy	Vax rates as UK	Vax rates as US	Earlier Start (2020/12/27)
<i>Sri Lanka</i>	10,469 [5,817 - 25,975]	12,278 [6,876 - 30,891]	12,022 [6,795 - 30,102]	7,072 [4,073 - 15,962]
<i>Morocco</i>	11,019 [5,631 - 21,795]	13,159 [6,527 - 27,219]	13,151 [6,539 - 26,960]	8,024 [4,245 - 15,142]
<i>Bolivia</i>	4,862 [3,916 - 6,279]	6,872 [5,590 - 8,879]	6,817 [5,551 - 8,761]	2,490 [1,975 - 3,235]
<i>Indonesia</i>	106,957 [76,428 - 180,817]	123,420 [89,451 - 208,587]	123,489 [89,456 - 208,555]	18,289 [12,649 - 30,110]
<i>Bangladesh</i>	88,371 [38,950 - 194,299]	103,508 [46,006 - 228,900]	101,747 [45,585 - 222,961]	14,413 [5,155 - 39,503]
<i>Ukraine</i>	19,337 [11,274 - 43,367]	32,169 [20,348 - 70,698]	31,236 [19,690 - 68,895]	5,969 [3,222 - 13,571]
<i>Mozambique</i>	16,735 [8,938 - 31,488]	18,857 [10,102 - 35,537]	19,546 [10,446 - 36,780]	6,825 [3,465 - 13,237]
<i>Kenya</i>	26,165 [13,432 - 51,182]	29,713 [15,723 - 56,088]	29,976 [15,801 - 56,907]	6,313 [3,039 - 13,253]

Table 4: Number of deaths averted with vaccination rates of high income countries (Italy, UK, US) and with earlier start of vaccination campaign (2020/12/27). The baseline are simulations with actual, data-driven vaccine rollouts. Median and 90% CI are reported. These figures account for underreporting of deaths, therefore they represent the real estimated avoided number of fatalities.

References

- [1] United nations, department of economic and social affairs, population division. world population prospects: The 2019 revision. <https://population.un.org/wpp/Download/Metadata/Documentation/>, 2020. Accessed: 2020-11-30.
- [2] COVID-19 Data Repository by the Center for Systems Science and Engineering (CSSE) at Johns Hopkins University. <https://github.com/CSSEGISandData/COVID-19>, 2021.
- [3] Global Dashbord for Vaccine Equity. <https://data.undp.org/vaccine-equity/>, 2021. Accessed: 2021-11-30.
- [4] Coronavirus (covid-19) vaccinations. <https://ourworldindata.org/covid-vaccinations>, 2020. Accessed: 2020-11-30.
- [5] Jantien A Backer, Don Klinkenberg, and Jacco Wallinga. Incubation period of 2019 novel coronavirus (2019-ncov) infections among travellers from wuhan, china, 20–28 january 2020. *Eurosurveillance*, 25(5), 2020.
- [6] Stephen M. Kissler, Christine Tedijanto, Edward Goldstein, Yonatan H. Grad, and Marc Lipsitch. Projecting the transmission dynamics of sars-cov-2 through the postpandemic period. *Science*, 368(6493):860–868, 2020.
- [7] Dina Mistry, Maria Litvinova, Ana Pastore y Piontti, Matteo Chinazzi, Laura Fumanelli, Marcelo F C Gomes, Syed A Haque, Quan-Hui Liu, Kunpeng Mu, Xinyue Xiong, M Elizabeth Halloran, Ira M Longini, Stefano Merler, Marco Ajelli, and Alessandro Vespignani. Inferring high-resolution human mixing patterns for disease modeling. *Nature Communications*, 12(1):323, 2021.
- [8] Robert Verity, Lucy Okell, Ilaria Dorigatti, Peter Winskill, Charles Whittaker, Natsuko Imai, Gina Cuomo-Dannenburg, Hayley Thompson, Patrick Walker, Han Fu, Amy Dighe, Jamie Griffin, Marc Baguelin, Sangeeta Bhatia, Adhiratha Boonyasiri, Anne Cori, Zulma M. Cucunubá, Rich FitzJohn, Katy Gaythorpe, and Neil Ferguson. Estimates of the severity of coronavirus disease 2019: a model-based analysis. *The Lancet Infectious Diseases*, 20, 03 2020.
- [9] Duygu Balcan, Bruno Gonçalves, Hao Hu, José J. Ramasco, Vittoria Colizza, and Alessandro Vespignani. Modeling the spatial spread of infectious diseases: The global epidemic and mobility computational model. *Journal of Computational Science*, 1(3):132 – 145, 2010.
- [10] Ben S Cooper, Richard J Pitman, W John Edmunds, and Nigel J Gay. Delaying the international spread of pandemic influenza. *PLoS Med*, 3(6):e212, 2006.
- [11] Julia Shapiro, Natalie E. Dean, Zachary J. Madewell, Yang Yang, M.Elizabeth Halloran, and Ira Longini. Efficacy estimates for various covid-19 vaccines: What we know from the literature and reports. *medRxiv*, 2021.
- [12] Edouard Mathieu, Hannah Ritchie, Esteban Ortiz-Ospina, Max Roser, Joe Hasell, Cameron Appel, Charlie Giattino, and Lucas Rodés-Guirao. A global database of COVID-19 vaccinations. *Nature Human Behaviour*, 5(7):947–953, 2021.
- [13] CoVariants. <https://covariants.org>, 2021.
- [14] Nextstrain. <https://nextstrain.org>, 2021.
- [15] Stefan Elbe and Gemma Buckland-Merrett. Data, disease and diplomacy: Gisaid’s innovative contribution to global health. *Global Challenges*, 1(1):33–46, 2017.
- [16] Baisheng Li, Aiping Deng, Kuibiao Li, Yao Hu, Zhencui Li, Qianling Xiong, Zhe Liu, Qianfang Guo, Lirong Zou, Huan Zhang, Meng Zhang, Fangzhu Ouyang, Juan Su, Wenzhe Su, Jing Xu, Huifang Lin, Jing Sun, Jinju Peng, Huiming Jiang, Pingping Zhou, Ting Hu, Min Luo, Yingtao Zhang, Huanying Zheng, Jianpeng Xiao, Tao Liu, Rongfei Che, Hanri Zeng, Zhonghua Zheng, Yushi Huang, Jianxiang Yu, Lina Yi, Jie Wu, Jingdiao Chen, Haojie Zhong, Xiaoling Deng, Min Kang, Oliver G. Pybus, Matthew Hall, Katrina A. Lythgoe, Yan Li, Jun Yuan, Jianfeng He, and Jing Lu. Viral infection and transmission in a large, well-traced outbreak caused by the sars-cov-2 delta variant. *medRxiv*, 2021.

- [17] Amanda Minter and Renata Retkute. Approximate bayesian computation for infectious disease modelling. *Epidemics*, 29:100368, 2019.
- [18] Mikael Sunnåker, Alberto Giovanni Busetto, Elina Numminen, Jukka Corander, Matthieu Foll, and Christophe Dessimoz. Approximate bayesian computation. *PLOS Computational Biology*, 9(1):1–10, 01 2013.
- [19] Centers for Disease Control and Prevention, COVID-19 Pandemic Planning Scenarios. <https://www.cdc.gov/coronavirus/2019-ncov/hcp/planning-scenarios.html#table-1>, 2021. Accessed 2021/02/02.
- [20] Google LLC "Google COVID-19 Community Mobility Reports". <https://www.google.com/covid19/mobility/>, 2020. Accessed: 2021-08-01.
- [21] EU Vaccination Days. <http://www.politicheeuropee.gov.it/en/communication/news/european-vaccination-days-against-covid-19/>, 2021. Accessed: 2021-06-10.
- [22] Nicolò Gozzi, Matteo Chinazzi, Jessica T. Davis, Kunpeng Mu, Ana Pastore y Piontti, Marco Ajelli, Nicola Perra, and Alessandro Vespignani. Anatomy of the first six months of covid-19 vaccination campaign in italy. *medRxiv*, 2021.
- [23] Valentina Marziano, Giorgio Guzzetta, Alessia Mammone, Flavia Riccardo, Piero Poletti, Filippo Trentini, Mattia Manica, Andrea Siddu, Antonino Bella, Paola Stefanelli, et al. The effect of covid-19 vaccination in italy and perspectives for living with the virus. *Nature communications*, 12(1):1–8, 2021.